# Problem Set #2

## Problem 1

(A) $N \sim L^D K^D$ (see equation 19 Chap. 5)

This refers to Kittel, not Simon

$$\mathcal{D}(\omega) = \frac{dN}{d\omega} = \frac{dN}{dk}\frac{dk}{d\omega} \cong L^D D K^{D-1}\frac{dK}{d\omega}$$

for a dispersion relation $\omega = AK^\alpha$

$$\frac{d\omega}{dK} = \alpha K^{\alpha-1} A$$

$$\mathcal{D}(\omega) \cong L^D \frac{D K^{D-1}}{\alpha K^{\alpha-1} A} \sim L^D \frac{D}{\alpha A} K^{D-\alpha}$$

$$K = \left(\frac{\omega}{A}\right)^{1/\alpha}$$

$$\mathcal{D}(\omega) \sim \frac{L^D D}{\alpha A}\left[\frac{\omega}{A}\right]^{\frac{D-\alpha}{\alpha}} = \frac{L^D D}{\alpha A}\left[\frac{\omega}{A}\right]^{\frac{D}{\alpha}-1}$$

$$C_V \cong \frac{1}{V}\frac{\partial}{\partial T}\int \frac{\mathcal{D}(\omega)\hbar\omega}{e^{\frac{\hbar\omega}{KT}}-1}\, d\omega$$

in low T limit $\frac{\hbar\omega}{KT} << 1 \Rightarrow \frac{1}{e^{\frac{\hbar\omega}{KT}}-1} \approx e^{-\frac{\hbar\omega}{K_B T}}$

$$C_V = \frac{1}{V}\frac{\partial}{\partial T}\int \frac{L^D D}{\alpha A}\left[\frac{\omega}{A}\right]^{\frac{D}{\alpha}-1} \hbar\omega\, e^{-\frac{\hbar\omega}{K_B T}}\, d\omega$$

let $x = \frac{\hbar\omega}{k_B T}$

$$C_V = \frac{1}{V}\frac{\partial}{\partial T}\frac{L^D D\,\hbar}{\alpha A^{D/\alpha}}\left[\frac{k_B T}{\hbar}\right]^{\frac{D}{\alpha}+1}\underbrace{\int_0^\infty x^{D/\alpha} e^{-x}\,dx}_{\text{number}}$$

$$\text{so } C_V \sim \frac{\partial}{\partial T} T^{\frac{D}{\alpha}+1} \quad \boxed{\sim T^{D/\alpha}}$$

(B)

Graphene $D = 2$

$\omega_1 = 24\,\text{km/s}\;k \quad \alpha = 1$

$\omega_2 = 18\,\text{km/s}\;k \quad \alpha = 1$

$\omega_3 = 6\times10^{-7}\frac{m^2}{s}k^2 \quad \alpha = 2$

each mode contributes to the heat capacity

$$C_1 \sim T^2\left(\frac{1}{24\,\text{km/s}}\right)^2 \times B_1$$

$$C_2 \sim T^2\left(\frac{1}{18\,\text{km/s}}\right)^2 \times B_1$$

$$C_3 \sim T\left(\frac{1}{6\times10^{-7}\frac{m^2}{s}}\right) \times B_2$$

where $B_1$ and $B_2$ are constants depending on $D$, $\hbar$, $k_B$ and factors of $\pi$

Unless $B_2 << B_1$ then $C_3$ will dominate as $\left(\frac{1}{6\times10^{7}\ m/s}\right)$ is >> $\left(\frac{1}{18\ km/s}\right)$

so the heat capacity of graphene should be linear in T at low T.

From the graph it appears that Graphene has a $C_V \sim 1.1 \frac{mJ}{g\ ^0K}(T)$

in good agreement.

Now for SWNT

$D = 1$

$\alpha = 1$ $\quad w_{1,2} = 9\ km/sec\ k$ ← 2 degenerate modes

$\alpha = 1$ $\quad w_3 = 15\ km/s\ k$

$\alpha = 1$ $\quad w_4 = 18\ km/s\ k$

Each mode contributes to $C_V$

$$C_{1,2} \sim T\left(\frac{1}{9\,km/sec}\right) \times B_3$$

$$C_3 \sim T\left(\frac{1}{15\,km/s}\right) \times B_3$$

$$C_4 \sim T\left(\frac{1}{18\,km/s}\right) \times B_3$$

$B_3$ is a constant (the same for all three $C_s$)

So $$C_{TOTAL} \sim B_3 \left[\frac{2}{9} + \frac{1}{15} + \frac{1}{18}\right] T$$

From the graph

$$C_{SWNT} \sim 6 \times 10^{-2} \frac{mJ}{g\,^\circ K} T^{1.7}$$ between 10 and 100°K

at lower energies however $T < 5K$

$$C_{SWNT} \sim T$$

So we get the expected answer at very low T, however for $T > 5K$

Other modes come into play and give us behavior indicative of crossover at a different $T/\alpha$.

These turn out to be modes associated with phonon vibrational modes quantized by the small radius of the nanotube.

You wouldn't know this from the given info, however the experimental data is a clue that something new must be happening.

Overall the $C_V$ of graphene dominates because the $\varepsilon k^2$ mode has such a low energy & very small. that there are plenty of occupied levels at low $T$ which translates to high $C$.

Solutions to Problem #2

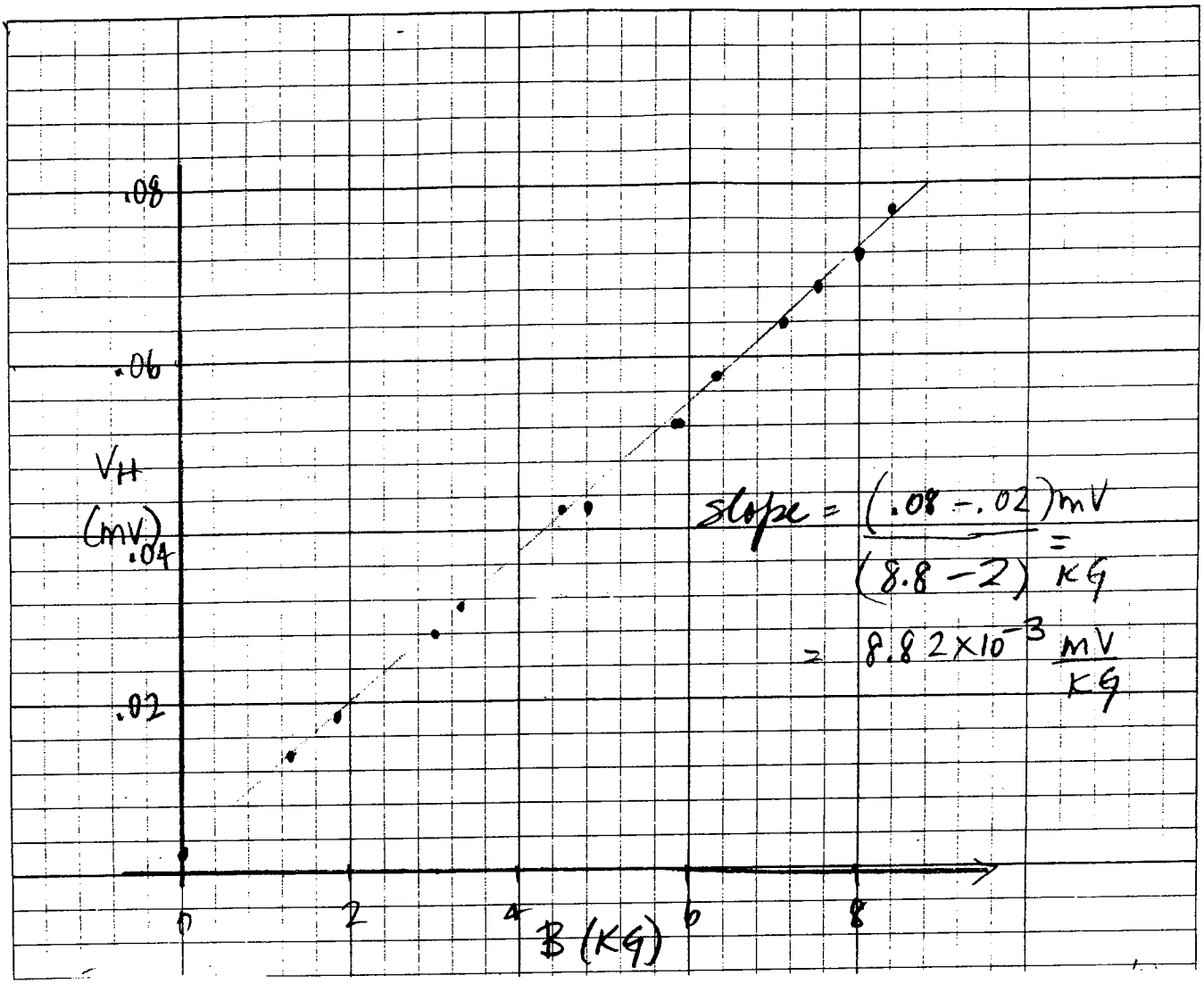

(A) Find $R_{Hall}$

From kittel $R_H = \dfrac{E_{Hall}}{j_x B}$

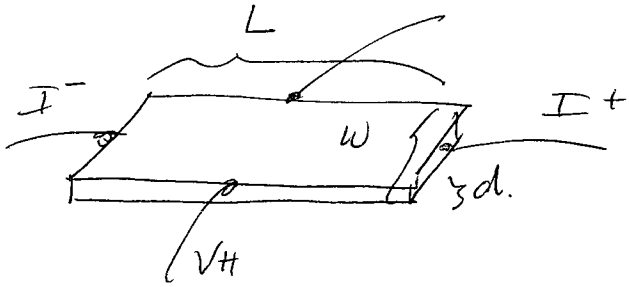


$$E_{Hall} = \frac{V_{Hall}}{w}$$

$$j_x = \frac{I}{wd}$$

$$R_H = \frac{E_{Hall}}{j_x B} = \frac{V_{Hall}\, wd}{w I B} = \frac{V_{Hall}\, d}{I B}$$

$$R_{Hall} = \frac{8.82\times10^{-3}\,mV}{KG}\ \frac{(2400\,\mathring{A})}{(.400\,mA)}$$

$10KG = \frac{Wb}{m^2}$

$$= \frac{8.82\times10^{-6}\,V}{1\times10^{-1}\,\frac{Wb}{m^2}}\ \frac{(2.4\times10^{-7}\,m)}{0.4\,A}$$

$$\boxed{R_{Hall} = 5.29\times10^{-11}\,\frac{m^3\,\Omega}{Wb}}$$

(B) $R_{Hall} = \dfrac{-1}{ne} \Rightarrow \text{units} \Rightarrow \dfrac{m^3}{\text{coulombs}}$

This means that $\dfrac{\Omega}{Wb} = \dfrac{1}{\text{coulombs}}$.

lets check this

Wb is flux ie. $B \cdot \text{Area} = \Phi$

Biot-Savart Law.

$$dF = I\, d\vec{l} \times \vec{B}$$

units $F = I l B$

$$qE = I l B$$

multiply by $l$ $\quad qEl = Il^2B = I\Phi$

$$El = V$$

$$\therefore \quad qV = \Phi I$$

$$\frac{V}{I\Phi} = \frac{1}{q}$$

$$\frac{\Omega}{Wb} = \frac{1}{\text{Coulombs}} \quad !$$ in MKS units.

$$\therefore R_H = 5.29 \times 10^{-11} \frac{m^3}{\text{Coulombs}} = \frac{1}{ne}$$

$$n = (R_H e)^{-1} = \left[(1.6 \times 10^{-19}\ \text{Coulombs}) \times \left(5.29 \times 10^{-11} \frac{m^3}{\text{Coul}}\right)\right]^{-1}$$

$$= 1.18 \times 10^{29}\ \frac{1}{m^3}$$

$n = 1.18 \times 10^{23} \frac{}{cm^3}$ ← # of electrons in sample / unit volume.

$N_A = 6.022 \times 10^{23} \frac{\text{atoms}}{\text{mole}}$.

$$\frac{\#}{\text{volume}} = 6.022 \times 10^{23} \frac{\text{atoms}}{\text{mole}} \times 8.96 \frac{g}{cc} \times \frac{\text{mole}}{63.55 g}$$

$$= 8.49 \times 10^{22}$$

$$\boxed{\frac{n_{exp}}{n_{actual}} = 1.4}$$

Compare to Kittels value for Hall coefficient

Cu. pg 167 Table 4

$$\frac{Cu\ \text{measured}}{Cu\ \text{calculated}} = \frac{-0.6}{-0.82} = .7317$$

n is inversely proportional to this so

$$\left(\frac{n_{exp}}{n_{calculated}}\right)_{Kittel} = \underline{1.366} \quad \text{we got } \underline{1.4}!$$

Simon 3.2

Scattering Times [NOTE!! The value of $\rho$ FROM PAGE 26 ARE SUPPOSED TO BE $10^{-8}\ \Omega m$ NOT $10^{8}\ \Omega m$]

$$\sigma = \frac{n e^2 \tau}{m} \qquad (3.2)$$

$n = \frac{\#\ \text{electrons}}{\text{volume}}$ $\quad e = 1.6\times10^{-19}\,C$ $\quad \sigma = \frac{1}{\rho}$ (in $B=0$)

$m = \frac{0.511\times10^{6}\ eV}{c^2}$ } a convenient way of writing $m_e$ when using $\Omega$ and $C$

$$n = \text{Density}\ (g/cm^3)\left(\frac{1}{\text{Z grams}}\right)\left(6.\times10^{23}\ \frac{\text{atom}}{\text{mole}}\right)\left(1\ \frac{\text{valence electron}}{\text{atom}}\right) = \frac{\text{electrons}}{cm^3}$$

Z grams ↑ atomic weight

$$n_e(Ag) = \frac{10.5\ g}{cm^3}\ \frac{1\ \text{mole}}{47\ g}\left(6\times10^{23}\ \frac{\text{atoms}}{\text{mole}}\right) = 1.34\times10^{23}\ \frac{e}{cm^3}$$

$$n_e(Li) = \frac{0.53\ g}{cm^3}\ \frac{1\ \text{mole}}{3g}\left(6\times10^{23}\ \frac{\text{atom}}{\text{mole}}\right) = 1.06\times10^{23}\ \frac{e}{cm^3}$$

---

$$\tau^{-1} = \frac{n e^2}{m\sigma} = \frac{n e^2 \rho}{m}$$

For (Ag) $\quad \tau = 1.34\times10^{23}\ \frac{\cancel{e}}{cm^3}\ (1.6\times10^{-19}\ \cancel{e})\ 1.59\times10^{-8}\ \Omega m\ (3\times10^{8})^2\ \frac{m^2}{\Omega}$ $\quad$ ($c^2$)

$$\frac{0.511\times10^{6}\ \cancel{e}\ V}$$

$$\frac{1}{\tau} = 6\times10^{7}\ \frac{m^3}{cm^3}\ \frac{10^{6}\,cm^3}{m^3} = 6\times10^{13}\ \frac{1}{s}$$

$C\Omega = V$

$\tau = 1.66\times10^{-14}\ sec$

For Li

$$\tau^{-1} = \frac{1.06\times10^{23}}{cm^3}\ (1.6\times10^{-19}C)\ e\ \frac{(9.28\times10^{-8}\,\Omega\cdot m)\,(3\times10^{8})^2\,\frac{m^2}{s^2}}{0.511\times10^{6}\,eV} \times \frac{10^6\,cm^3}{m^3}$$

$$\tau = 3.6\times10^{-15}\,sec$$

---

Now for Nitrogen

$$\tau = \frac{1}{n\langle v\rangle\,\sigma}$$

let $\sigma = \pi d^2 = \pi(0.37\times10^{-9}m)^2$

$$\langle v\rangle = \sqrt{\frac{8\,K_B T}{\pi m}}$$

m for Nitrogen = $14\,m_p = 14(1.67\times10^{-27}kg)$

$K_B T$ in Joules at Room temp (300°K) $= 4.11\times10^{-21}\,J$

$$\langle v\rangle = \sqrt{\frac{8\,(4.11\times10^{-21}J)}{\pi\,(14)(1.67\times10^{-27}kg)}} = 2.37\times10^{2}\,m/s$$

$n_{gas\ density} = 1.25\times10^{-3}\,g/cc$ at STP

but we need $\frac{\#\ of\ atoms}{cc}$ each atom $14(1.67\times10^{-27}kg)$

so $1.25\times10^{-3}\frac{g}{cc}\ \frac{1}{(14)(1.67\times10^{-27}g)} = 5.35\times10^{22}\frac{atoms}{cc}$

$$\tau = \frac{1}{n\langle v\rangle \sigma} = \left[\frac{1}{5.35\times10^{22}\ \frac{\text{atoms}}{\text{cm}^3}} \quad \frac{1}{2.37\times10^{2}\ \frac{\text{m}}{\text{s}}} \quad \frac{1}{\pi(0.37\times10^{-9}\ \text{m})^2}\right]$$

$$= 1.8\times10^{-7}\ \text{s}\ \frac{\text{cm}^3}{\text{m}^3} \times \frac{\text{m}^3}{10^6\ \text{cm}^3}$$

$$\tau = 1.8\times10^{-13}\ \text{sec for Nitrogen gas}$$

The scattering time is about 1-2 orders of magnitude smaller for the metals compared to gaseous nitrogen.

So there is less scattering of an $N_2$ in air compared to an electron in a typical metal.

3.3

electrons { $n_e$ and $\tau_e$
$m_e$ and $-e$

free ions { $n_i$ and $\tau_i$
$m_i$ and $+e$

(A) Resistivity:

Actually conductivity is easier since both the free electrons and ions work in parallel you can just add the conductivities

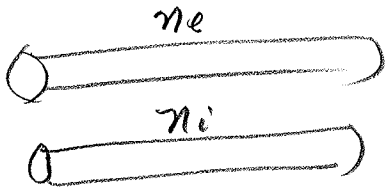


It's like having 2 wires one of electrons and one of ions, and you can have current flow through either.

$$\sigma = \sigma_e + \sigma_i$$

$$\sigma_{TOTAL} = \frac{n_e e^2 \tau_e}{m_e} + \frac{n_i e^2 \tau_i}{m_i}$$

$$\rho_{TOTAL} = \frac{1}{\sigma_{TOTAL}} \text{ (when } B=0) = \left[ \frac{n_e e^2 \tau_e}{m_e} + \frac{n_i e^2 \tau_i}{m_i} \right]^{-1}$$

(B) Assume Wiedemann Franz law

then $K = LT\sigma$

$$= \frac{3}{2}\left(\frac{k_B}{e}\right)^2 T \left[\frac{n_e e^2 \tau_c}{m_e} + \frac{n_i e^2 \tau_i}{m_i}\right]^{-1}$$

(C) You were not asked to do (C)

But here is the solution

**The following is from the physics dept at Oxford but I don't know who the instructor was.**

# Handout 11

# Magnetoresistance in three-dimensional systems

## 11.1 Introduction

Magnetoresistance is a general term for the changes in the components of the resistivity and conductivity tensors of materials caused by the application of magnetic field. We are going to treat the magnetoresistance of metals in a quite general and simple manner. First, however, the Hall effect in a system with more than one type of carrier will be described, as it helps to illuminate the more general discussion of metals that will follow, and gives a clue as to the origins of magnetoresistance.

## 11.2 Hall effect with more than one type of carrier

### 11.2.1 General considerations

We consider the Hall effect with two or more carrier types present (*e.g.* electrons and holes). The geometry of a Hall effect measurement is shown in Figure 11.1; the magnetic field $\mathbf{B}$ is applied parallel to the $z$ direction (*i.e.* $\mathbf{B} = (0, 0, B)$), whilst the current $I$ is driven through the sample in the $x$ direction. The electric field $\mathbf{E}$ is assumed to be $\mathbf{E} = (E_x, E_y, 0)$; we assume that any effect is going to occur in the plane perpendicular to $\mathbf{B}$ because of the nature of the Lorentz force (see Equation 11.1 below). Voltage measuring contacts are provided on the sample so that $E_x$ and $E_y$ can be deduced (see Figure 11.1).

We assume that the drift velocity $\mathbf{v}$ of each species of carrier can be treated using the Relaxation Time Approximation, *i.e.*

$$m^*\{\frac{\mathrm{d}\mathbf{v}}{\mathrm{d}t} + \frac{\mathbf{v}}{\tau}\} = q\mathbf{E} + q\mathbf{v} \times \mathbf{B}, \tag{11.1}$$

where $q$ is the charge of the carrier, $m^*$ is its effective mass (assumed isotropic and energy-independent) and $\tau^{-1}$ is its relaxation (scattering) rate. Note that all changes in $\mathbf{v}$ occur in the plane perpendicular to $\mathbf{B}$; therefore it is sufficient to split Equation 11.1 into $x$ and $y$ components to give

$$m^*\{\frac{\mathrm{d}v_x}{\mathrm{d}t} + \frac{v_x}{\tau}\} = qE_x + qv_yB \tag{11.2}$$

and

$$m^*\{\frac{\mathrm{d}v_y}{\mathrm{d}t} + \frac{v_y}{\tau}\} = qE_y - qv_xB. \tag{11.3}$$

The Hall effect represents a steady state of the system, *i.e.* $\mathrm{d}v_x/\mathrm{d}t = \mathrm{d}v_y/\mathrm{d}t = 0$. Substituting Equation 11.2 into Equation 11.3 with $\mathrm{d}v_x/\mathrm{d}t = \mathrm{d}v_y/\mathrm{d}t = 0$ gives

$$\frac{m^*v_y}{\tau} = qE_y - \frac{qB\tau}{m^*}\{qE_x + qv_yB\}, \tag{11.4}$$

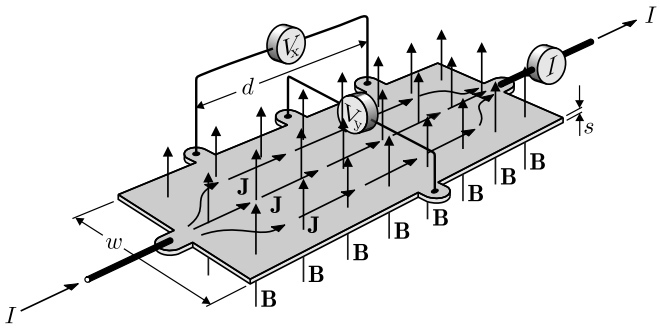


Figure 11.1: Geometry of a Hall effect measurement on a sample of thickness $s$ and width $w$. On entering the sample, the current $I$ becomes a current density $\mathbf{J}$ of average magnitude $I/ws$. The magnetic field (flux density) is uniform within the sample. The positions of voltmeters for measuring $E_x = V_x/d$ and $E_y = V_y/w$ are shown symbolically.

which can be rearranged to give

$$v_y\{\frac{m^*}{\tau} + \frac{q^2B^2\tau}{m^*}\} = qE_y - \frac{q^2B\tau}{m^*}E_x. \tag{11.5}$$

Dividing through by $m^*/\tau$ and making the identification $eB/m^* \equiv \omega_c$ (*i.e.* the cyclotron frequency) gives

$$v_y\{1 + \omega_c^2\tau^2\} = \frac{q\tau}{m^*}\{E_y - \omega_c\tau E_x\}. \tag{11.6}$$

Hall effect experiments are usually quite deliberately carried out at low magnetic fields, such that $\omega_c\tau \ll 1$, implying that terms $\sim \omega_c^2\tau^2$ can be neglected. Therefore Equation 11.6 becomes

$$v_y = \frac{q\tau}{m^*}\{E_y - \omega_c\tau E_x\} = \frac{q\tau}{m^*}\{E_y - \frac{qB\tau}{m^*}E_x\}. \tag{11.7}$$

We now consider an arbitrary number of carrier types, with each type being labelled by the integer $j$; the $j$th carrier type has effective mass $m_j^*$, charge $q_j$, scattering rate $\tau_j$ and number density $n_j$. For each carrier type, Equation 11.7 therefore becomes

$$v_{y,j} = \frac{q_j\tau_j}{m_j^*}\{E_y - \frac{q_jB\tau_j}{m_j^*}E_x\}. \tag{11.8}$$

Now the net transverse current must be zero, as there is nowhere for it to go (see Figure 11.1). Therefore

$$\sum_j n_j v_{y,j} q_j = 0. \tag{11.9}$$

Equations 11.8 and 11.9 can be used to derive the Hall coefficient for an arbitrary number of carrier types. We shall use them to treat the simple case of electrons and heavy holes in a semiconductor; as usual, the light holes, with their relatively feeble density of states compared to that of the heavy holes, will be ignored.

### 11.2.2 Hall effect in the presence of electrons and holes

In the case of electrons in the conduction band (with effective mass $m_c^*$, scattering rate $\tau_c^{-1}$, charge $q_c$, density $n$) and heavy holes in the valence band (with effective mass $m_{hh}^*$, scattering rate $\tau_{hh}^{-1}$, charge $q_{hh}$, density $p$), Equations 11.8 and 11.9 combine to give

$$\frac{nq_c^2\tau_c}{m_c^*}\{E_y - \frac{q_cB\tau_c}{m_c^*}E_x\} + \frac{pq_{hh}^2\tau_{hh}}{m_{hh}^*}\{E_y - \frac{q_{hh}B\tau_{hh}}{m_{hh}^*}E_x\} = 0. \tag{11.10}$$

Equation 11.10 can be rearranged to give

$$E_y\{n\mu_c + p\mu_{hh}\} = E_x\{p\mu_{hh}^2 - n\mu_c^2\}B, \tag{11.11}$$

where $\mu_{hh} = |q_{hh}\tau_{hh}/m_{hh}^*|$ is the heavy hole mobility and where $\mu_c = |q_c\tau_c/m_c^*|$ is the electron mobility, and I have substituted $q_{hh} \equiv +e$ and $q_c \equiv -e$. Now

$$E_x = \frac{J_x}{\sigma} = \frac{J_x}{|e|(n\mu_c + p\mu_{hh})}, \tag{11.12}$$

where $J_x$ is the current density in the $x$ direction. Combining Equations 11.11 and 11.12 gives

$$R_H \equiv \frac{E_y}{J_x B} = \frac{1}{|e|}\frac{(p\mu_{hh}^2 - n\mu_c^2)}{(n\mu_c + p\mu_{hh})^2}. \tag{11.13}$$

This treatment is explored in more depth in the Problems.[1]

### 11.2.3 A clue about the origins of magnetoresistance

Equations 11.9 and 11.10 show that, although no *net* current flows in the $y$ direction, the currents carried in the $y$ direction by a particular type of carrier may (*i.e.* probably will) be non-zero. Carriers flowing in the $y$ direction will experience a Lorentz force caused by $\mathbf{B}$ in the *negative $x$ direction* (you can satisfy yourself that this will always be the case). This backflow of carriers will act to change the apparent resistivity $E_x/J_x$, *i.e.* cause magnetoresistance.[2]

In the following Section we shall explore this idea more formally and in a very general manner. We shall see that the presence of more than one "carrier type" (and here the term is used very imprecisely) is necessary for magnetoresistance to be observed.

In order to treat all of the different contributions to the conductivity and resistivity in a sanitary fashion, we shall introduce the idea of conductivity and resistivity tensors.

## 11.3 Magnetoresistance in metals

### 11.3.1 The absence of magnetoresistance in the Sommerfeld model of metals

We consider first of all a metal with a simple spherical Fermi surface and isotropic, energy-independent effective mass. As in Section 11.2.1, the magnetic field $\mathbf{B}$ will be parallel to $z$ (see Figure 11.1), and we shall use the same symbols (effective mass $m^*$, scattering rate $\tau^{-1}$ and electronic charge $-e$). Applying Equation 11.1, we have

$$m^*\{\frac{d\mathbf{v}}{dt} + \frac{\mathbf{v}}{\tau}\} = -e\mathbf{E} - e\mathbf{v}\times\mathbf{B}. \tag{11.14}$$

Two things may be deduced from this equation.

- The motion of the electrons in the direction parallel to $\mathbf{B}$ is unaffected. Therefore there will be *no longitudinal magnetoresistance*; in this context, the longitudinal resistivity is measured in the direction parallel to the field $\mathbf{B}$ (*i.e.* both the applied current density and the measured electric field are parallel to $\mathbf{B}$).

- There may well be *transverse magnetoresistance*. Here *transverse* resistivity means that measured in the direction perpendicular to the field $\mathbf{B}$ (*i.e.* both the applied current density and the measured electric field are in the plane perpendicular to $\mathbf{B}$).

[1] Some excellent illustrative data are shown in Figure 4.3 of *Semiconductor Physics*, by K. Seeger (Springer, Berlin 1991).

[2] Those who are unconvinced by this hand-waving argument should go back to Equation 11.6 and repeat the above derivation for $\omega_c\tau \gg 1$. They will find that $((p/\mu_{hh}) + (n/\mu_c))E_y = (p-n)E_xB$ (*i.e* the Hall field is zero if $n = p$). Putting $n = p$ yields $J_x = ((p/\mu_{hh}) + (n/\mu_c))eE_x/B^2$, *i.e.* $\rho \propto B^2$. This is the reason for the very large magnetoresistance in compensated semimetals (equal number of holes and electrons at Fermi surface) such as Bi.


Figure 11.2: Geometrical interpretation of the components of current density $J_x$, $J_y$ and caused by electric field component $E_x$ and magnetic field $(0, 0, B)$; **J** is the total current density.

Let us look at the second point in more detail. To simplify matters, we shall initially consider an electric field directed only along the $x$ direction (*i.e.* $\mathbf{E} = (E_x, 0, 0)$); our tactic will be to deduce the components of the current density $\mathbf{J} = (J_x, J_y, 0)$ that flow in response to **B** and **E**.

As in the previous Section, we are dealing with a steady state of the system, *i.e.* $\mathrm{d}v_x/\mathrm{d}t = \mathrm{d}v_y/\mathrm{d}t = 0$. Taking $\mathbf{B} = (0, 0, B)$ and $\mathbf{E} = (E_x, 0, 0)$ as defined above, we rewrite Equation 11.2 and Equation 11.3 in the form

$$v_{\mathrm{d},x} = -\frac{e\tau}{m^*}\{E_x + v_{\mathrm{d},y}B\} \tag{11.15}$$

and

$$v_{\mathrm{d},y} = \frac{e\tau}{m^*}v_{\mathrm{d},x}B, \tag{11.16}$$

where the subscript "d" emphasises the fact that we are dealing with a drift velocity.

Equations 11.15 and 11.16 show that the magnetic field has made the conductivity anisotropic; it has become a tensor, rather than a scalar. In order to work out the components of the *conductivity tensor*, we look at the current densities $J_x = -nev_{\mathrm{d},x}$ and $J_y = -nev_{\mathrm{d},y}$. Substituting these into Equations 11.15 and 11.16 yields, after some rearrangement

$$J_x = \sigma_{xx}E_x \text{ and } J_y = \sigma_{yx}E_x,$$

where

$$\sigma_{xx} = \frac{\sigma_0}{1 + \omega_{\mathrm{c}}^2\tau^2} \tag{11.17}$$

and

$$\sigma_{yx} = \frac{\sigma_0\omega_{\mathrm{c}}\tau}{1 + \omega_{\mathrm{c}}^2\tau^2}. \tag{11.18}$$

Here $\sigma_0 = ne^2\tau/m^*$ is the zero-field conductivity in the Sommerfeld model and $\omega_{\mathrm{c}} = eB/m^*$ is the cyclotron frequency.

The conductivity tensor shows that, in a magnetic field, the total current density **J** no longer flows parallel to the applied $E$-field, $E_x$; instead, it now contains both $x$ and $y$ components. Figure 11.2 gives a geometrical interpretation of **J** and the components of current density $J_x$, $J_y$ caused by electric field component $E_x$ and magnetic field $(0, 0, B)$.

Equation 11.17 shows that as $B \to \infty$, $\sigma_{xx} \propto B^{-2}$. We might therefore expect to see some magnetoresistance. However, most experiments (see Figure 11.1) measure *voltages* dropped in the $x$ and $y$ directions between pairs of contacts, rather than measuring the $x$ and $y$ components of the current density. In such experiments the current is forced to go along the $x$ direction, so that $\mathbf{J} \equiv J_x\mathbf{e}_1$; in contrast, the electric field will have components in both $x$ and $y$ directions (see Figure 11.3). Therefore we want the components

$$\rho_{xx} \equiv \frac{E_x}{J_x} \text{ and } \rho_{yx} \equiv \frac{E_y}{J_x} \tag{11.19}$$

of the *resistivity* tensor, rather than the conductivity.

The general conductivity tensor is

$$\sigma = \begin{pmatrix} \sigma_{xx} & \sigma_{yx} \\ \sigma_{xy} & \sigma_{yy} \end{pmatrix}. \tag{11.20}$$

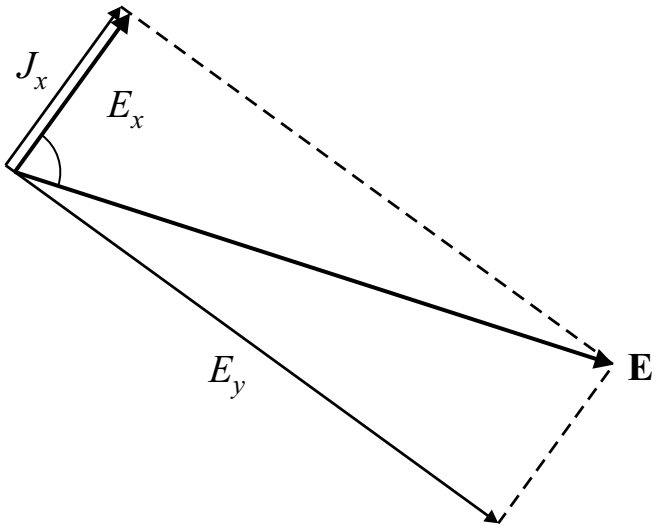


Figure 11.3: Geometrical interpretation of the components of electric field $E_x$, $E_y$ and the total field $\mathbf{E}$ caused by current density component $J_x$ and magnetic field $(0, 0, B)$.

The derivations which start at Equations 11.15 and 11.16 can be repeated with $\mathbf{E} = (0, E_y, 0)$ to yield $\sigma_{xy} = -\sigma_{yx}$ and $\sigma_{yy} = \sigma_{xx}$,[3] so that we have

$$\sigma = \begin{pmatrix} \sigma_{xx} & -\sigma_{xy} \\ \sigma_{xy} & \sigma_{xx} \end{pmatrix} = \frac{\sigma_0}{1 + \omega_c^2 \tau^2} \begin{pmatrix} 1 & \omega_c \tau \\ -\omega_c \tau & 1 \end{pmatrix}. \tag{11.21}$$

This tensor can then be inverted using standard methods to give the resistivity tensor

$$\rho = \begin{pmatrix} \rho_{xx} & \rho_{yx} \\ \rho_{xy} & \rho_{yy} \end{pmatrix} = \frac{1}{\sigma_0} \begin{pmatrix} 1 & -\omega_c \tau \\ \omega_c \tau & 1 \end{pmatrix}. \tag{11.22}$$

The components of interest in the experimental arrangement shown in Figure 11.1 are

$$\rho_{xx} = \rho_0 \text{ and } \rho_{yx} = -\rho_0 \omega_c \tau = -\frac{B}{ne}, \tag{11.23}$$

where $\rho_0 = 1/\sigma_0$ (see Figure 11.3). Therefore we get no magnetoresistance in the diagonal components of the resistivity tensor and the familiar Hall effect for one carrier in the off-diagonal components.

### 11.3.2 The presence of magnetoresistance in real metals

Almost all real metals exhibit some form of magnetoresistance, and so we must try to find out what is wrong with the approach above. In the above derivation we assumed that all carriers had the same value of $m^*$ and $\tau$. However in a real metal we could have

- electrons with different values of $m^*$ (*e.g.* from anisotropic bands);
- electrons with different values of $\tau$ (*e.g.* some parts of the Fermi surface may have higher scattering probabilities than others);
- a combination of both.

We therefore split the current density $\mathbf{J}$ into several components

$$\mathbf{J}_j = \sigma_{xx,j} E_x \mathbf{e}_1 + \sigma_{yx,j} E_y \mathbf{e}_2 \tag{11.24}$$

[3] This fact can also be deduced using symmetry considerations.

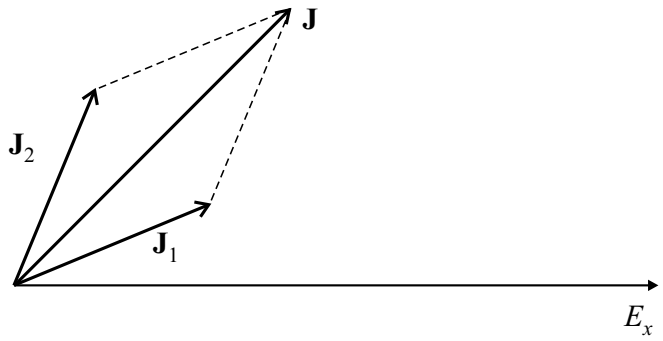


Figure 11.4: Geometrical interpretation of the components of current density $\mathbf{J}_1$ and $\mathbf{J}_2$ due to two different species of carrier caused by electric field component $E_x$ and magnetic field $(0, 0, B)$.

where the index $j$ indicates a contribution from the $j$th type of carrier. Each type of carrier will have a different density $n_j$ and/or effective mass $m_j^*$ and/or scattering rate $\tau_j^{-1}$. Hence, the components of the conductivity tensor $\sigma_{xx,j}$ and $\sigma_{yx,j}$ will differ for each type of carrier, resulting in $\mathbf{J}_j$s which do not in general point in the same direction as each other.

The total current $\mathbf{J}$ is just the sum of all of the components

$$\mathbf{J} = \sum_j \mathbf{J}_j. \tag{11.25}$$

In order to see what happens, we take a very simple case of just two carrier types, $j = 1, 2$. Equation 11.24 shows that, barring some very unlikely coincidence, $\mathbf{J}_1$ and $\mathbf{J}_2$ will be in different directions. This situation is illustrated in Figure 11.4; the application of the magnetic field means that $\mathbf{J}_1$ and $\mathbf{J}_2$ are no longer parallel, so that

$$|\mathbf{J}| \leq |\mathbf{J}_1 + \mathbf{J}_2|, \tag{11.26}$$

*i.e.* the resistivity increases with increasing magnetic field. We therefore have magnetoresistance.

We note in passing that, as above, $\sigma_{xx} \propto B^{-2}$ as $B \to \infty$ (see Equation 11.17 and the paragraph following it). This will be important in the discussion of the following section.

### 11.3.3 The use of magnetoresistance in finding the Fermi surface shape

We consider first a *closed* section of Fermi surface, about which a carrier can perform closed orbits under the influence of a magnetic field (see Figure 11.5). As $B \to \infty$, $\omega_c\tau \to \infty$, so that an electron will tend to make many circuits of the Fermi surface before scattering. Therefore, the velocity of the electron in the plane perpendicular to $\mathbf{B}$ will average to zero; this is the reason why $\sigma_{xx}$ and $\sigma_{yy}$ both vary as $B^{-2}$ in very high fields. Using the conductivity tensor components, the current densities can be written

$$J_x = \sigma_{xx}E_x + \frac{1}{RB}E_y \tag{11.27}$$

and

$$J_y = -\frac{1}{RB}E_x + \sigma_{yy}E_y \tag{11.28}$$

where $R$ is the Hall coefficient, and the off-diagional tensor components have been written $\sigma_{xy} = 1/RB$ and $\sigma_{yx} = -1/RB$. Eliminating $E_y$ gives

$$E_x = \frac{1}{\sigma_{xx} + (R^2B^2\sigma_{yy})^{-1}}J_x + \frac{RB}{1 + R^2B^2\sigma_{xx}\sigma_{yy}}J_y. \tag{11.29}$$

As mentioned above, $\sigma_{xx}$ and $\sigma_{yy}$ both vary as $B^{-2}$ in very high fields, so that as $B \to \infty$, $(B^2R^2\sigma_{yy})^{-1} \gg \sigma_{xx}$. Therefore, $\rho_{xx} = E_x/J_x$ tends to a constant at high fields, *i.e.* it *saturates*.

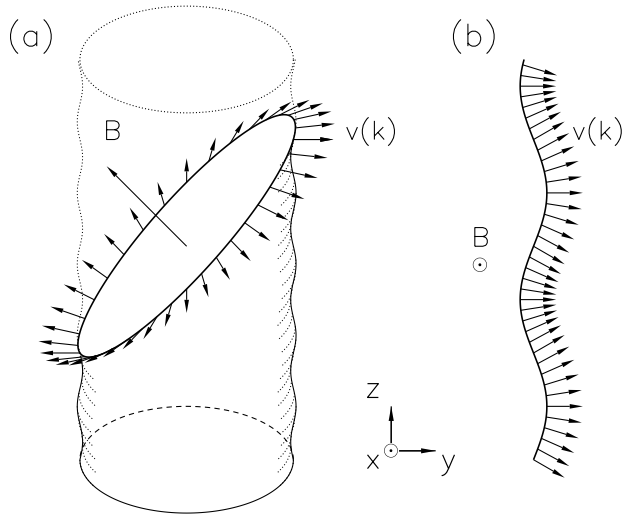


Figure 11.5: (a) Schematic of electron motion on a closed section of Fermi surface in a magnetic field. The arrows indicate the velocities of an electron following a closed orbit about the Fermi surface in a plane perpendicular to the magnetic field **B**. (b) An open orbit on the Fermi surface. In an in-plane magnetic field, electrons will be driven across the Fermi surface, so that their velocities (shown by arrows) will rock from side to side.

We now turn to an *open* section of Fermi surface (see Figure 11.5) about which an electron cannot perform closed orbits under the influence of a magnetic field. In this case, even as $B \to \infty$, the average value of $v_y$ remains finite; therefore $\sigma_{yy} \to C$, a constant. Substituting $\sigma_{yy} = C$ and $\sigma_{xx} = AB^{-2}$, where $A$ is another constant, into Equation 11.29 yields

$$\rho_{xx} = \frac{E_x}{J_x} = \frac{1}{AB^{-2} + (R^2B^2C)^{-1}} \propto B^2, \tag{11.30}$$

*i.e.* $\rho_{xx} \propto B^2$ as $B \to \infty$.

We therefore have two distinct results

- **closed orbits** produce a $\rho_{xx}$ which saturates as $B \to \infty$;
- **open orbits** produce a $\rho_{xx}$ proportional to $B^2$ as $B \to \infty$.

This has been used to great effect in elucidating the Fermi surface of metals such as Copper, where changing the orientation of the magnetic field can produce open or closed orbits about the Fermi surface (see Figure 11.6).

## 11.4 The magnetophonon effect

Oscillations can be observed in the resistivity of both bulk and two-dimensional semiconductors at elevated temperatures $\sim 100$ K; this is known as *the magnetophonon effect* or *magnetophonon resonance*. The effect is caused by resonant inter-Landau-level scattering of electrons by long-wavelength longitudinal optic (LO) phonons; such phonons are very effective scatterers of electrons. (Why? think about the type of polarisation field that they produce.) As such phonons have virtually zero wavevector, the transition is "vertical", *i.e.* between almost identical points in $k$-space in the initial and final Landau levels involved. By conservation of energy, the condition for the magnetophonon effect to occur is therefore

$$j\omega_c = \omega_{LO}, \tag{11.31}$$

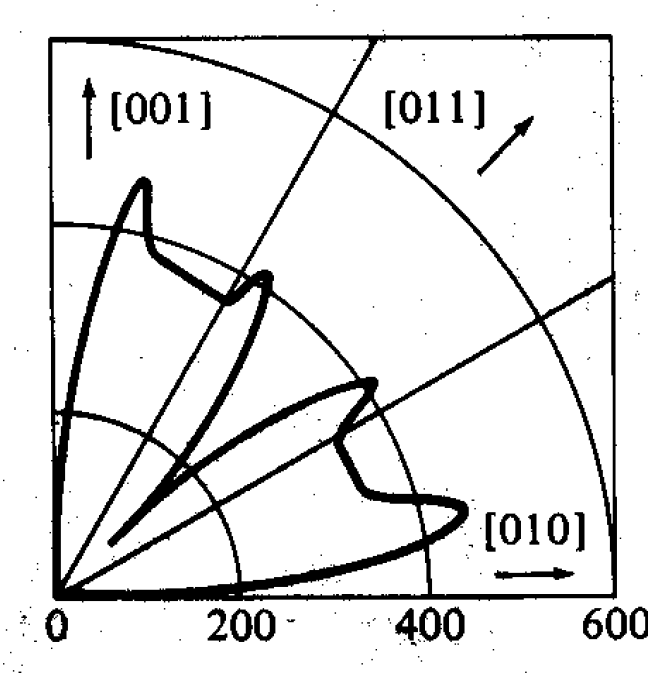


Figure 11.6: Magnetoresistance of Copper at a temperature of 4.2 K and a fixed magnetic field of 1.8 T; the current has been applied in the [100] direction (perpendicular to the plane of the page) and the magnetic field has been rotated from the [001] direction to the [010] direction. The magnetoresistance has been plotted radially as $(\rho(B) - \rho(B = 0))/\rho(B = 0)$. (Data from J.R. Klauder and J.E. Kunzler, *The Fermi Surface*, edited by W. Harrison (Wiley, New York, 1960.)

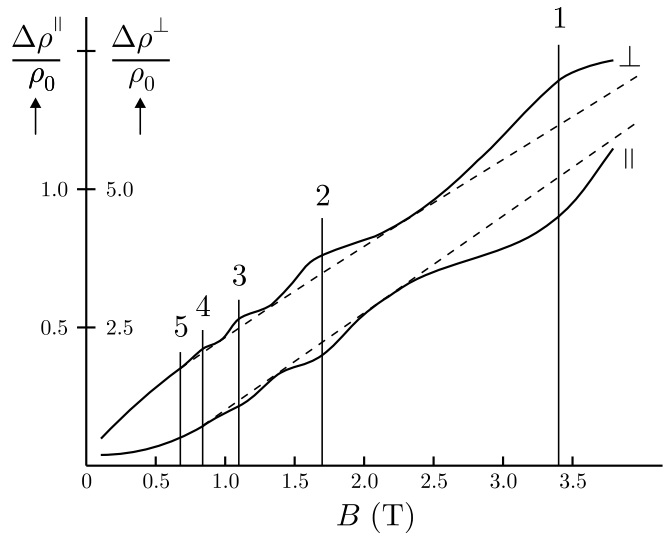


Figure 11.7: Magnetophonon resonances in the longitudinal and transverse resistvities of InSb at 90 K.

where $\omega_{\rm LO}$ is the phonon frequency, *i.e.* an integer number $j$ of Landau level spacings matches an LO phonon energy. This leads to oscillations in the resistivity periodic in $1/B$; if the phonon frequency is known, the effective mass can be deduced from Equation 11.31.

The conditions for magnetophonon resonance to be observed are

- the temperature should be low enough for the Landau levels to be resolved;
- the temperature should be high enough for a substantial population of LO phonons.

In practice, 70-100 K seems to be a good compromise. Figure 11.7 shows magnetophonon resonances in InSb at 90 K.

## 11.5 Reading

Some useful general reading on magnetoresistance is contained in *Electrons in Metals and Semiconductors*, by R.G. Chambers (Chapman and Hall, London 1990) Chapters 1, 2 and 11, *Semiconductor Physics*, by K. Seeger (Springer, Berlin 1991) Chapter 9 (hard), *Solid State Physics*, by N.W Ashcroft and N.D. Mermin (Holt, Rinehart and Winston, New York 1976) Chapters 12, 13 and 15 (hard).